Nonlin. Processes Geophys. Discuss., https://doi.org/10.5194/npg-2018-25
Manuscript under review for journal Nonlin. Processes Geophys.
Discussion started: 2 May 2018

Nonlinear Processes in Geophysics
Discussions
Open Access
EGU

Fluctuations of finite-time Lyapunov exponents in an intermediate-complexity atmospheric model: a multivariate and large-deviation perspective

Frank Kwasniok

College of Engineering, Mathematics and Physical Sciences, University of Exeter, North Park Road, Exeter EX4 4QF, United Kingdom

Correspondence: Frank Kwasniok (F.Kwasniok@exeter.ac.uk)

Abstract. The stability properties as characterised by the fluctuations of finite-time Lyapunov exponents around their mean values are investigated in a three-level quasi-geostrophic atmospheric model with realistic mean state and variability. An empirical orthogonal function (EOF) analysis of the fluctuation field of all of the finite-time Lyapunov exponents is performed. The two leading modes are patterns where the most unstable Lyapunov exponents fluctuate in phase. These modes are independent of the integration time of the finite-time Lyapunov exponents. Then large-deviation rate functions are estimated from time series of daily Lyapunov exponents using the Legendre transform and from time series of Lyapunov exponents with long integration times based on their probability density function. Serial correlation in the time series is properly accounted for. Convergence to a large-deviation principle can be established for all of the Lyapunov exponents which is rather slow for the most unstable exponents and becomes faster when going further down in the Lyapunov spectrum. Convergence is generally faster for the Gaussian behaviour in the vicinity of the mean value. The curvature of the rate functions at the minimum is linked to the corresponding elements of the diffusion matrix. Also joint large-deviation rate functions beyond the Gaussian approximation are calculated for the first and the second Lyapunov exponent.

1 Introduction

The atmosphere is a high-dimensional nonlinear chaotic dynamical system; its time evolution is characterised by sensitivity to initial conditions (Lorenz, 1963; Kalnay, 2003). As a consequence predictability is limited; small errors in the initial states progressively grow under the time evolution until the forecast eventually becomes useless, that is, indistinguishable from the invariant measure or climatology of the system. Understanding the structure of this inherent instability is key to improve forecasts at all timescales.

Sensitivity to initial conditions and perturbation growth in nonlinear dynamical systems are often quantified using Lyapunov exponents (e.g., Eckmann and Ruelle, 1985; Ott, 2002; Pikovsky and Politi, 2016). They describe the asymptotic growth or decay of infinitesimal perturbations. A system is chaotic if it has at least one positive Lyapunov exponent. However, the predictability properties may vary substantially across state space. Finite-time or local Lyapunov exponents allow a characterisation of the stability of a particular initial state with respect to a predefined prediction horizon.

Nonlin. Processes Geophys. Discuss., https://doi.org/10.5194/npg-2018-25
Manuscript under review for journal Nonlin. Processes Geophys.
Discussion started: 2 May 2018

Nonlinear Processes in Geophysics
Discussions
Open Access
EGU

Lyapunov exponents have been calculated for various geophysical fluid systems, ranging from highly truncated atmospheric models (Legras and Ghil, 1985), to intermediate-complexity atmospheric models (Vannitsem and Nicolis, 1997; Schubert and Lucarini, 2015), to coupled atmosphere-ocean models (Vannitsem and Lucarini, 2016). A review has been published recently by Vannitsem (2017). Models tuned to realistic conditions turn out to possess quite a large number of positive Lyapunov exponents corresponding to a high-dimensional chaotic attractor.

The present paper investigates the fluctuations of finite-time Lyapunov exponents in an intermediate-complexity atmospheric model with realistic mean state and variability. It focuses on two aspects which have so far found little attention in the context of geophysical fluid systems. Firstly, the covariance structure of the fluctuation field is studied by means of a principal component analysis. Secondly, we are looking at the large-deviation behaviour of the finite-time Lyapunov exponents at long integration times.

The paper is organised as follows: In section 2 the atmospheric model is described. The methodology which consists of calculating Lyapunov exponents, the multivariate fluctuation analysis and the large-deviation theory is outlined in sections 3, 4 and 5. The results are presented and discussed in section 6. Some conclusions are drawn in section 7.

2 The atmospheric model

A quasi-geostrophic (QG) three-level model on the sphere is used here as dynamical framework. The model is the same as introduced by Kwasniok (2007) except for the horizontal resolution and the coefficient of hyperviscosity. A very similar model was introduced by Marshall and Molteni (1993). The dynamical equations are

$$\frac{\partial q_i}{\partial t} + J(\Psi_i, q_i) = D_i + S_i, \qquad i = 1,2,3 \tag{1}$$

where Ψ_i and q_i are the streamfunction and the potential vorticity at level i and J denotes the Jacobian operator on the sphere. All variables are nondimensional using the radius of the earth as the unit of length and the inverse of the angular velocity of the earth as the unit of time. The three pressure levels are located at 250, 500 and 750 hPa. Potential vorticity and the streamfunction are related by

$$q_1 = \nabla^2\Psi_1 - R_{1,2}^{-2}(\Psi_1 - \Psi_2) + 2\mu \tag{2}$$

$$q_2 = \nabla^2\Psi_2 + R_{1,2}^{-2}(\Psi_1 - \Psi_2) - R_{2,3}^{-2}(\Psi_2 - \Psi_3) + 2\mu \tag{3}$$

$$q_3 = \nabla^2\Psi_3 + R_{2,3}^{-2}(\Psi_2 - \Psi_3) + 2\mu + h \tag{4}$$

where μ is the sine of geographic latitude. The Rossby deformation radii $R_{1,2}$ and $R_{2,3}$ have dimensional values of 575 km and 375 km. The h represents a nondimensional topography which is related to the actual dimensional topography of the earth h^* by $h = 2\mu_0 h^*/H$, where μ_0 is the sine of an average geographic latitude taken to be 45N and H is a scale height set to 8 km.

Nonlin. Processes Geophys. Discuss., https://doi.org/10.5194/npg-2018-25
Manuscript under review for journal Nonlin. Processes Geophys.
Discussion started: 2 May 2018

The dissipative terms are given as

$$D_1 = k_{\mathrm{N}} R_{1,2}^{-2}(\Psi_1 - \Psi_2) - k_{\mathrm{H}} \nabla^8 \hat{q}_1 \tag{5}$$

$$D_2 = -k_{\mathrm{N}} R_{1,2}^{-2}(\Psi_1 - \Psi_2) + k_{\mathrm{N}} R_{2,3}^{-2}(\Psi_2 - \Psi_3) - k_{\mathrm{H}} \nabla^8 \hat{q}_2 \tag{6}$$

$$D_3 = -k_{\mathrm{N}} R_{2,3}^{-2}(\Psi_2 - \Psi_3) - k_{\mathrm{E}} \nabla^2 \Psi_3 - k_{\mathrm{H}} \nabla^8 \hat{q}_3 \tag{7}$$

They are Newtonian temperature relaxation, Ekman damping on the lowest level, and a strongly scale-selective horizontal diffusion of vorticity and temperature. The $\hat{q}_i$ is the time-dependent part of the potential vorticity at level i, that is, $\hat{q}_1 = q_1 - 2\mu$, $\hat{q}_2 = q_2 - 2\mu$ and $\hat{q}_3 = q_3 - 2\mu - h$. The coefficient of temperature relaxation, k_{N}, represents a radiative timescale of 25 days; the Ekman drag damps the streamfunction at 750 hPa on a spindown timescale of 1.5 days. The coefficient of horizontal diffusion is such that harmonics of total wavenumber 21 are damped at a timescale of 1.5 days. The terms S_1, S_2 and S_3 are diabatic sources of potential vorticity which are independent of time but spatially varying.

The model is considered on the northern hemisphere. The boundary condition of no meridional flow, that is, vanishing streamfunction, is applied at the equator on all three model levels. The horizontal discretization is spectral, triangularly truncated at total wavenumber 21. The number of degrees of freedom is 231 for each level and $N = 693$ in total. The model is integrated in time using the third-order Adams-Bashforth scheme with a constant step size of 1 h.

In order to get a model behaviour close to that of the real atmosphere, the forcing terms are determined from ECMWF reanalysis data by requiring that when computing potential vorticity tendencies for a large number of observed atmospheric fields, the average of these tendencies must be zero (Roads, 1987). See Kwasniok (2007) for details on the parameter tuning procedure.

3 Lyapunov exponents

We consider a nonlinear autonomous dynamical system with state vector $\mathbf{x} = (x_1, \ldots, x_N)^{\mathrm{T}}$ governed by the evolution equations

$$\frac{d\mathbf{x}}{dt} = \mathbf{f}(\mathbf{x}). \tag{8}$$

The linearised dynamics of a small perturbation $\delta\mathbf{x}$ are given as

$$\frac{d}{dt}\delta\mathbf{x} = \frac{\partial \mathbf{f}}{\partial \mathbf{x}}\delta\mathbf{x}. \tag{9}$$

The propagation between times t_0 and t can be written as

$$\delta\mathbf{x}(t) = \mathbf{M}(t_0, t)\delta\mathbf{x}(t_0) \tag{10}$$

where $\mathbf{M}$ is the resolvent matrix. If the system is ergodic then according to the theorem by Oseledets (1968) the limit

$$\mathbf{S} = \lim_{t\to\infty} (\mathbf{M}^{\mathrm{T}}\mathbf{M})^{\frac{1}{2(t-t_0)}} \tag{11}$$

Nonlin. Processes Geophys. Discuss., https://doi.org/10.5194/npg-2018-25
Manuscript under review for journal Nonlin. Processes Geophys.
Discussion started: 2 May 2018

Nonlinear Processes in Geophysics
Discussions
Open Access
EGU

exists and is the same for almost all initial conditions $\mathbf{x}(t_0)$. The (global) Lyapunov exponents are defined as

$$\lambda_j = \log \sigma_j \tag{12}$$

where σ_j are the positive eigenvalues of the matrix $\mathbf{S}$. The set of all Lyapunov exponents is called the Lyapunov spectrum. The Lyapunov exponents are independent of norm.

In order to characterise perturbation growth or decay over a finite integration time τ the finite-time or local Lyapunov exponents $\Lambda_j^{(\tau)}(\mathbf{x}_0)$ are introduced. They are here calculated using the standard algorithm based on the Gram-Schmidt orthogonalisation (Shimada and Nagashima, 1979; Benettin et al., 1980). An ensemble of perturbations is initialised and integrated forward in time together with the full nonlinear model. After integration time τ the perturbations are re-orthonormalised using a QR-decomposition. The finite-time Lyapunov exponents are then given as

$$\Lambda_j^{(\tau)}(\mathbf{x}_0) = \frac{1}{\tau} \log R_{jj}(t_0, t_0 + \tau) \tag{13}$$

where R_{jj} are the diagonal elements of the triangular matrix in the QR-decomposition. The finite-time Lyapunov exponents depend on the norm chosen in the Gram-Schmidt orthogonalisation procedure. We here use the total energy norm.

The finite-time Lyapunov exponents are related to the global Lyapunov exponents by $\lim_{\tau\to\infty} \Lambda_j^{(\tau)}(\mathbf{x}_0) = \lambda_j$ for almost all $\mathbf{x}_0$ and $\langle \Lambda_j^{(\tau)} \rangle = \lambda_j$ for all τ where $\langle \cdot \rangle$ denotes an ensemble average over initial conditions on the attractor of the system.

4 Multivariate fluctuation analysis

The correlations between the fluctuations of the finite-time Lyapunox exponents are studied by means of an empirical orthogonal function (EOF) analysis based on the scaled covariance matrix $\mathbf{D}^{(\tau)}$ defined as

$$D_{j,k}^{(\tau)} = \left\langle \Lambda_j^{(\tau)} \Lambda_k^{(\tau)} - \lambda_j \lambda_k \right\rangle \tau \tag{14}$$

where $\langle \cdot \rangle$ denotes an ensemble average over the attractor of the system which is here estimated as a mean over a long time series. In the limit of large integration time τ we expect convergence to the diffusion matrix $\mathbf{D}$ (Kuptsov and Politi, 2011; Pikovsky and Politi, 2016):

$$D_{j,k} = \lim_{\tau\to\infty} D_{j,k}^{(\tau)} \tag{15}$$

The vector of global Lyapunov exponents is defined as $\lambda = (\lambda_1, \ldots, \lambda_N)^{\mathrm{T}}$ and the fluctuation field as $\Lambda^{(\tau)} = (\Lambda_1^{(\tau)}, \ldots, \Lambda_N^{(\tau)})^{\mathrm{T}}$. The eigenvalues and eigenvectors of the symmetric, positive definite matrix $\mathbf{D}^{(\tau)}$ are calculated:

$$\mathbf{D}^{(\tau)} \mathbf{e}_j^{(\tau)} = \mu_j \mathbf{e}_j^{(\tau)} \tag{16}$$

The fluctuation field of the FTLEs is expanded as

$$\Lambda^{(\tau)} = \lambda + \sum_{j=1}^{N} z_j \mathbf{e}_j^{(\tau)} \tag{17}$$

Nonlin. Processes Geophys. Discuss., https://doi.org/10.5194/npg-2018-25
Manuscript under review for journal Nonlin. Processes Geophys.
Discussion started: 2 May 2018

with $z_j = \left(\mathbf{e}_j^{(\tau)}\right)^{\mathrm{T}} \Lambda^{(\tau)}$. The eigenvectors are orthogonal,

$$\left(\mathbf{e}_j^{(\tau)}\right)^{\mathrm{T}} \mathbf{e}_k^{(\tau)} = \delta_{jk}; \tag{18}$$

the principal components are uncorrelated and their variance is given by the corresponding eigenvalue:

$$\langle z_j z_k \rangle = \mu_j \delta_{jk} \tag{19}$$

5 Large-deviation theory for FTLEs

Large-deviation theory (Kifer, 1990; Touchette, 2009) is a powerful approach from statistical physics for estimating the probability of rare events with many applications. It has recently been applied to the behaviour of finite-time Lyapunov exponents at long integration times (Kuptsov and Politi, 2011; Laffargue et al., 2013; Johnson and Meneveau, 2015). Large-deviation theory is in the following briefly described in the form in which it is used in the present study.

For a sequence of n independent and identically distributed (i. i. d.) random variables, $\{X_i\}_{i=1}^n$, the sample mean

$$S_n = \frac{1}{n} \sum_{i=1}^{n} X_i \tag{20}$$

is an unbiased estimator of and converges to the true mean, $\langle X \rangle$, as $n \to \infty$. By Cramér's theorem, for large n, the probability of large deviations of the sample mean from the true mean $\langle X \rangle$ behaves as

$$p(S_n = x) \sim \exp[-nI(x)] \tag{21}$$

where $I(x)$ is the large-deviation rate function or Cramér function, which is independent of n. The large-deviation rate function is given by the Legendre transform

$$I(x) = \sup_t [tx - K(t)] \tag{22}$$

with the cumulant generating function

$$K(t) = \log M(t) \tag{23}$$

and the moment generating function

$$M(t) = \left\langle e^{tX} \right\rangle \tag{24}$$

Large-deviation theory can be heuristically extended to FTLEs, which can be regarded as estimators of the global Lyapunov exponents. In the limit of large integration time τ, the probability density function of the FTLE $\Lambda_j^{(\tau)}$ is given as

$$p\left(\Lambda_j^{(\tau)} = x\right) \sim \exp[-\tau I_j(x)] \tag{25}$$

Nonlin. Processes Geophys. Discuss., https://doi.org/10.5194/npg-2018-25
Manuscript under review for journal Nonlin. Processes Geophys.
Discussion started: 2 May 2018

with a large-deviation rate function $I_j(x)$ which is independent of τ.

There are two ways of estimating the large-deviation rate functions $I_j(x)$ from data. By inverting eq.(25) we have

$$I_j(x) = -\lim_{\tau\to\infty} \frac{1}{\tau} \log p\left(\Lambda_j^{(\tau)} = x\right) \tag{26}$$

One would now calculate $I_j(x)$ from the probability density function of $\Lambda_j^{(\tau)}$ for various large values of τ and look for convergence. Alternatively, $I_j(x)$ can be determined from the Legendre transform based on a time series of FTLEs with some reference integration time τ_r:

$$\hat{I}_j(x) = \sup_t [tx - K_j(t)] \tag{27}$$

The cumulant generating function is estimated by the sample mean

$$K_j(t) = \log\left(\frac{1}{n}\sum_{k=1}^{n} e^{t\Lambda_{j,k}^{(\tau_\mathrm{r})}}\right) \tag{28}$$

For the maximisation over t it turns out to be sufficient to calculate $tx - K_j(t)$ on a fine enough grid and take the maximum value attained but an exact gradient-based maximisation could also be implemented easily. In view of eq.(21) the two estimates $I_j(x)$ and $\hat{I}_j(x)$ should be linked by

$$I_j(x) = \frac{\hat{I}_j(x)}{\tau_\mathrm{r} l_\mathrm{c}} \tag{29}$$

where l_c is a (dimensionless) correlation length reflecting the fact that FTLEs display serial correlation rather than being independent random variables. The correlation length is here specified as

$$l_\mathrm{c} = 1 + 2\sum_{i=1}^{\infty} \rho_i \tag{30}$$

where ρ_i is the autocorrelation of the time series of FTLEs with integration time τ_r at lag i. This particular definition of correlation length can be shown to be the correct one to deal with serial correlation in the Gaussian case where large-deviation theory degenerates to the central limit theorem. It is here heuristically adopted also for the general non-Gaussian case. Note that in order to establish a large-deviation principle with the probability density based method it is not necessary to specify any correlation length; however, in order to link the two different estimates of the large-deviation rate function it needs to be specified. The choice of the reference integration time τ_r is in principle arbitrary but a smaller value allows to determine the large-deviation rate function over a larger range of x values as more values are actually observed in the tails of the distribution. We here take $\tau_\mathrm{r} = 1$ day.

In the vicinity of the mean value λ_j the large-deviation rate function can be approximated by a second-order Taylor expansion as

$$I_j(x) = \frac{1}{2} q_j (x - \lambda_j)^2 \tag{31}$$

Nonlin. Processes Geophys. Discuss., https://doi.org/10.5194/npg-2018-25
Manuscript under review for journal Nonlin. Processes Geophys.
Discussion started: 2 May 2018

with

$$q_j = \left. \frac{d^2 I_j}{dx^2} \right|_{x=\lambda_j} \tag{32}$$

This in fact corresponds to a Gaussian probability density with mean λ_j and variance $1/(\tau q_j)$ which links the curvature of the rate function at the minimum with the diffusion matrix as

$$D_{j,j} = \frac{1}{q_j} \tag{33}$$

The large-deviation analysis can be extended to a multivariate approach (Kuptsov and Politi, 2011; Johnson and Meneveau, 2015). For large integration time τ the joint probability density function of all of the FTLEs of the system is given as

$$p(\Lambda^{(\tau)} = \mathbf{x}) \sim \exp[-\tau S(\mathbf{x})] \tag{34}$$

where $S(\mathbf{x})$ is the joint large-deviation rate function or joint Cramér function which is independent of τ.

There are again two methods of estimating the joint rate function. Firstly, it can be estimated from the joint probability density function as

$$S(\mathbf{x}) = -\lim_{\tau \to \infty} \frac{1}{\tau} p(\Lambda^{(\tau)} = \mathbf{x}) \tag{35}$$

Secondly, the joint rate function can be determined from the time series of FTLEs with integration time τ_r via the multivariate Legendre transform

$$\hat{S}(\mathbf{x}) = \sup_{\mathbf{t}} [\mathbf{t}^\mathrm{T} \mathbf{x} - K(\mathbf{t})] \tag{36}$$

with the joint cumulant generating function estimated by

$$K(\mathbf{t}) = \log \left(\frac{1}{n} \sum_{k=1}^{n} e^{\mathbf{t}^\mathrm{T} \Lambda_k^{(\tau_\mathrm{r})}} \right) \tag{37}$$

The two estimates of the rate function should be linked by

$$S(\mathbf{x}) = \frac{\hat{S}(\mathbf{x})}{\tau_\mathrm{r} l_\mathrm{c}} \tag{38}$$

where here it is not completely clear how to specify an appropriate correlation length.

Again, in the vicinity of the minimum the joint rate function can be approximated by the quadratic Taylor expansion

$$S(\mathbf{x}) = \frac{1}{2} (\mathbf{x} - \lambda)^\mathrm{T} \mathbf{Q} (\mathbf{x} - \lambda) \tag{39}$$

with

$$Q_{j,k} = \left. \frac{\partial^2 S}{\partial x_j \partial x_k} \right|_{\mathbf{x}=\lambda} \tag{40}$$

Nonlin. Processes Geophys. Discuss., https://doi.org/10.5194/npg-2018-25
Manuscript under review for journal Nonlin. Processes Geophys.
Discussion started: 2 May 2018

This amounts to a multivariate Gaussian joint probability density function with mean λ and covariance matrix $(\tau\mathbf{Q})^{-1}$ and gives a link to the diffusion matrix as

$$D_{j,k} = (\mathbf{Q}^{-1})_{j,k} \tag{41}$$

In high-dimensional systems it is usually too ambitious a task to determine $S(\mathbf{x})$ beyond the Gaussian approximation for the full system. The multivariate analysis described above is equally valid for any K-dimensional subset of FTLEs with $1 \leq K \leq N$ where $K = N$ corresponds to the full system and $K = 1$ recovers the univariate analysis. We here restrict ourselves to the bivariate case $K = 2$.

6 Results

6.1 Lyapunov exponents

Figure 1 displays the spectrum of global Lyapunov exponents of the QG model. The Lyapunov exponents were calculated as averages over a time series of 20000 days of daily finite-time Lyapunov exponents. There are 91 positive Lyapunov exponents. The largest Lyapunov exponent is estimated as $\lambda_1 = 0.344$/day, corresponding to an e-folding time of perturbation growth of 2.9 days which appears to be realistic for the real atmosphere. The spectrum starts off quite steep and then flattens at the near-zero exponents. For example, there are 69 Lyapunov exponents between 0.05/day and -0.05/day. The spectrum becomes steeper again at the trailing very stable exponents. Overall, there is a continuous spectrum of timescales with no clear timescale separation.

Figure 2 shows the standard deviation of the fluctuations of the finite-time Lyapunov exponents around their mean values. The standard deviation decreases with increasing integration time τ more or less uniformly for all exponents. The fluctuations are largest for the leading Lyapunov exponents and then quickly decrease. Slightly surprisingly they increase again towards the end of the Lyapunov spectrum with a particularly sharp increase for the most stable exponents at the very end of the spectrum. It is unclear if this is due to the definition of the finite-time Lyapunov exponents via the Gram-Schmidt orthogonalisation procedure and if it would also be observed for the finite-time Lyapunov exponents defined by making reference to the covariant Lyapunov vectors.

6.2 Multivariate fluctuation analysis

Figure 3 shows the explained variance and the cumulative explained variance of the principal components of the scaled Lyapunov fluctuations. There are five leading modes, then the eigenvalue spectrum sharply flattens off. The fraction of variance explained by the leading modes increases with increasing integration time τ. Going from $\tau = 1$ day to $\tau = 5$ days, the variance explained by the first principal component increases from 5% to almost 10% and the variance explained by the second principal component increases from about 2% to about 4%. However, due to the flatness of the bulk of the eigenvalue spectrum, even at $\tau = 5$ days a substantial number of modes is necessary to explain large parts of the fluctuation variance.

Nonlin. Processes Geophys. Discuss., https://doi.org/10.5194/npg-2018-25
Manuscript under review for journal Nonlin. Processes Geophys.
Discussion started: 2 May 2018

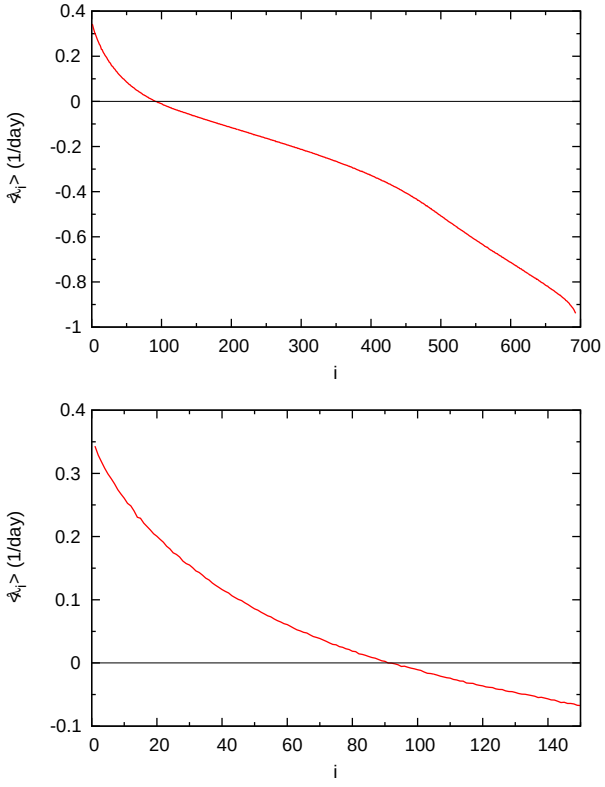

Figure 1. (a) Lyapunov spectrum of the QG model. (b) Close-up of (a).

In Figure 4 the structure of the two leading EOFs is displayed. Both modes are identical for all considered values of τ up to statistical sampling fluctuations. The first EOF shows a pattern where all of the leading finite-time Lyapunov exponents fluctuate together. This incorporates all of the positive exponents and extends beyond. Then there is a negative correlation with the dissipative Lyapunov modes in the second half of the Lyapunov spectrum. In the second EOF again the leading Lyapunov exponents fluctuate in phase; this here encompasses about the first 40 exponents. Then there is some negative correlation with the weakly dissipative Lyapunov modes and substantial positive correlation with the strongly dissipative exponents at the end of the Lyapunov spectrum.

6.3 Large-deviation analysis

6.3.1 One-dimensional approach

We now investigate whether the fluctuations of the finite-time Lyapunov exponents obey a large deviation principle. As representative examples we look at the first and the fifth Lyapunov exponent as two strongly unstable directions, at the zero exponent and at a weakly dissipative Lyapunov mode. The large-deviation rate function is calculated from the time series of $\Lambda_j^{(\tau)}$ with

Nonlin. Processes Geophys. Discuss., https://doi.org/10.5194/npg-2018-25
Manuscript under review for journal Nonlin. Processes Geophys.
Discussion started: 2 May 2018

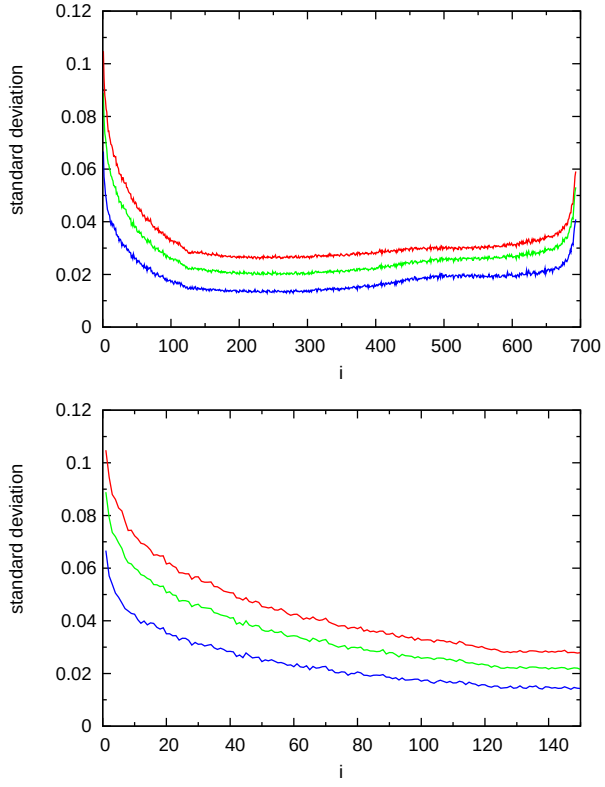

Figure 2. (a) Standard deviation of the fluctuations of the finite-time Lyapunov exponents for $\tau = 1$ day (red), $\tau = 2$ days (green) and $\tau = 5$ days (blue). (b) Close-up of (a).

$\tau = 1$ day using the Legendre transform and from the probability density of time series of $\Lambda_j^{(\tau)}$ for various larger values of τ. Then the corresponding element $D_{j,j}$ of the diffusion matrix is estimated from the curvature of the two estimates of the rate function as well as by calculating $D_{j,j}^{(\tau)}$ directly from the time series of $\Lambda_j^{(\tau)}$. The results are presented in Figures 5–8.

For the first LE the large-deviation rate function shows marked departure from Gaussian behaviour. Convergence to a large-deviation principle is observed but it is rather slow. At $\tau = 10$ days and even slightly visible at $\tau = 20$ days the mode of the probability density is still shifted away from the mean. Some convergence among the probability density based estimates is reached at $\tau = 30$ days; discrepancies with the estimate from the Legendre transform remain. The scaled variance of the time series of $\Lambda_1^{(\tau)}$ converges quite fast to a limiting value which coincides with the estimate obtained from the Legendre transform. Convergence is reached at about $\tau = 10$ days. The estimates from the probability density based rate functions are also converged at about $\tau = 10$ days, but to a lower value. This corresponds to the discrepencies between the rate functions visible in panel 5a, in particular the larger curvature at the minimum. A reason might be a non-optimal choice of the correlation time τ_c; using a slightly smaller value would bring the estimates closer together.

Nonlin. Processes Geophys. Discuss., https://doi.org/10.5194/npg-2018-25
Manuscript under review for journal Nonlin. Processes Geophys.
Discussion started: 2 May 2018

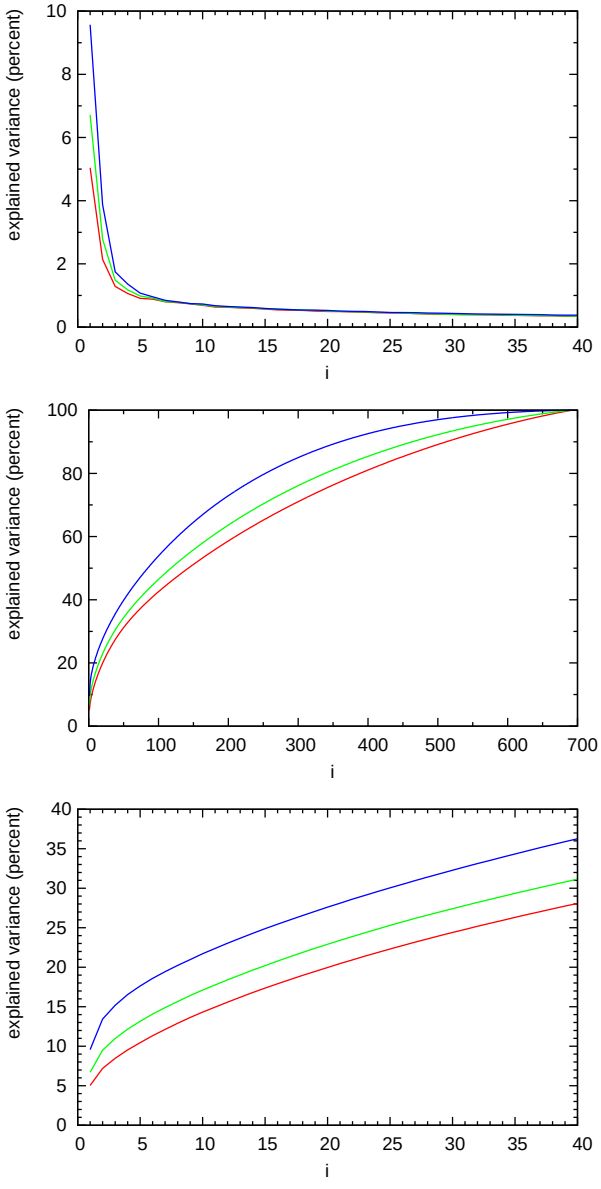

Figure 3. (a) Explained variance of the principal components of the finite-time Lyapunov fluctuations for $\tau = 1$ day (red), $\tau = 2$ days (green) and $\tau = 5$ days (blue). (b) Cumulative explained variance for $\tau = 1$ day (red), $\tau = 2$ days (green) and $\tau = 5$ days (blue). (c) Close-up of (b).

For the fifth Lyapunov exponent, non-Gaussian behaviour is clearly visible but it is less pronounced than for the first exponent. Convergence to a large-deviation principle can be observed at between $\tau = 20$ days and $\tau = 30$ days. The accordance between the estimate based on the Legendre transform and the estimates based on the probability density is very close here. Also the estimates of the diffusion coefficient $D_{5,5}$ are close together and show convergence at about $\tau = 15$ days.

Nonlin. Processes Geophys. Discuss., https://doi.org/10.5194/npg-2018-25
Manuscript under review for journal Nonlin. Processes Geophys.
Discussion started: 2 May 2018

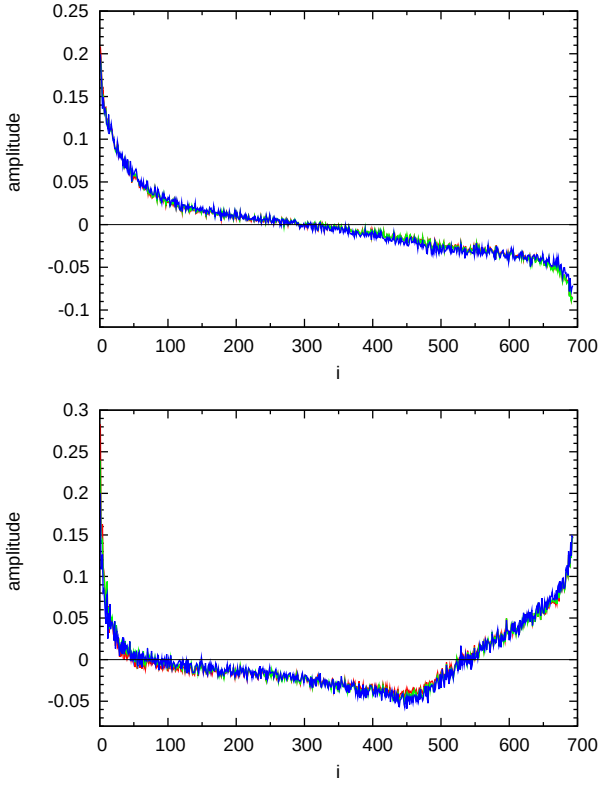

Figure 4. First (a) and second (b) empirical orthogonal function of the finite-time Lyapunov fluctuations for $\tau = 1$ day (red), $\tau = 2$ days (green) and $\tau = 5$ days (blue).

The zero exponent displays only small deviations from Gaussianity. Very good convergence to a large-deviation principle is observed which is markedly faster than for the positive LEs. The two different estimates of the rate function are very close together with almost perfect agreement in the vicinity of the mean value. Correspondingly, the different estimates of the diffusion coefficient $D_{92,92}$ are in close agreement and the convergence is fast.

For the 200th LE, the deviations of the rate function from Gaussian behaviour are even smaller. The convergence to a large-deviation principle is excellent and fast. The same holds for the estimates of the element $D_{200,200}$ of the diffusion matrix.

6.3.2 Two-dimensional approach

As an example of a multivariate large-deviation analysis Figure 9 shows the joint large-deviation rate function as obtained with the two-dimensional Legendre transform from the daily time series of the FTLEs as well as two estimates based on the joint probability density for $\tau = 15$ days and $\tau = 30$ days. The estimates of the diffusion coefficients $D_{1,1}$, $D_{2,2}$ and $D_{1,2}$ are also shown. The joint large-deviation rate function displays markedly non-Gausian behaviour and some dependence between $\Lambda_1^{(\tau)}$ and $\Lambda_2^{(\tau)}$. The two estimates based on the joint probability density show some convergence and agree with the estimates from

Nonlin. Processes Geophys. Discuss., https://doi.org/10.5194/npg-2018-25
Manuscript under review for journal Nonlin. Processes Geophys.
Discussion started: 2 May 2018

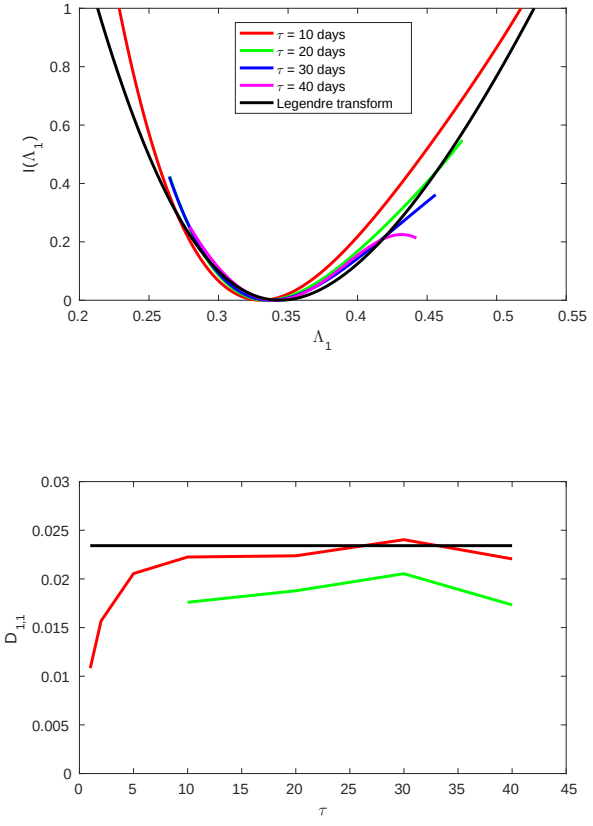

Figure 5. (a) Large-deviation rate function of the first finite-time Lyapunov exponent. (b) Element $D_{1,1}$ of the diffusion matrix as estimated from the time series of finite-time Lyapunov exponents (red), from the curvature of the large-deviation rate function derived from the probability density (green) and from the curvature of the large-deviation rate function derived with the Legendre transform (black).

the Legendre transform. Expectedly, the deviations in detail are larger than in the one-dimensional case as the estimate of the joint probability density is not very accurate given the limited data. For the element $D_{1,1}$, there is good agreement between the scaled variance of the time series of $\Lambda_1^{(\tau)}$ and the estimates based on the curvature of the rate function from the Legendre transform. The values from the curvature of the rate function based on the probability density are systematically lower but the discrepancy is smaller than in the one-dimensional case (Figure 5). For $D_{2,2}$ and the off-diagonal element $D_{1,2}$, there is very good agreement between the time series estimates and the estimates from the rate function based on the probability density. The values from the curvature of the rate function based on the Legendre transform are somewhat too large and too small, respectively. It is not immediately clear where this difference stems from.

Nonlin. Processes Geophys. Discuss., https://doi.org/10.5194/npg-2018-25
Manuscript under review for journal Nonlin. Processes Geophys.
Discussion started: 2 May 2018

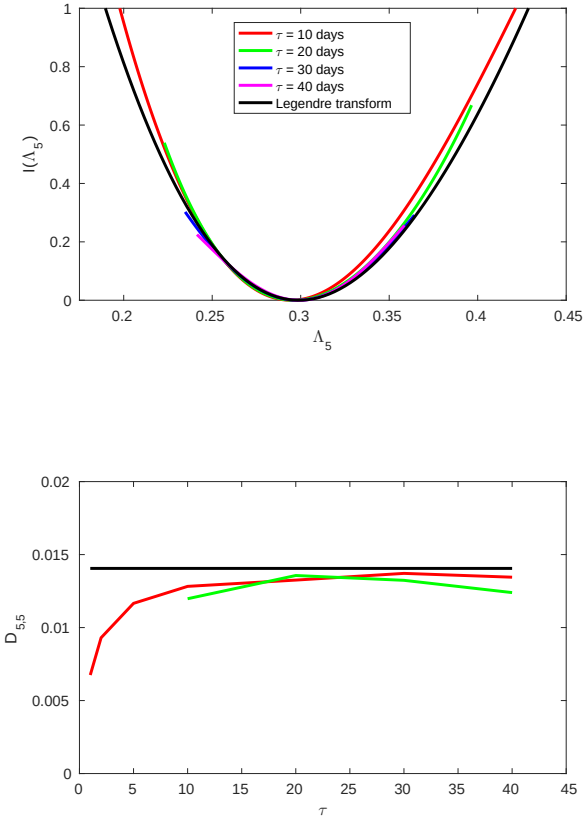

Figure 6. (a) Large-deviation rate function of the fifth finite-time Lyapunov exponent. (b) Element $D_{5,5}$ of the diffusion matrix as estimated from the time series of finite-time Lyapunov exponents (red), from the curvature of the large-deviation rate function derived from the probability density (green) and from the curvature of the large-deviation rate function derived with the Legendre transform (black).

7 Conclusions

The statistical properties of the fluctuations of FTLEs were investigated in a three-level quasi-geostrophic atmospheric model with realistic mean state and variability. The Lyapunov spectrum of the model has almost 100 positive LEs and displays no clear timescale separation.

A principal component analysis of the fluctuations of the FTLEs around their mean values was performed. The covariance matrix of the fluctuations is converged to the limiting diffusion matrix at about $\tau = 15$ days. There are substantial correlations among the different FTLEs. The first two empirical orthogonal functions are patterns where the leading positive FTLEs fluc-

Nonlin. Processes Geophys. Discuss., https://doi.org/10.5194/npg-2018-25
Manuscript under review for journal Nonlin. Processes Geophys.
Discussion started: 2 May 2018

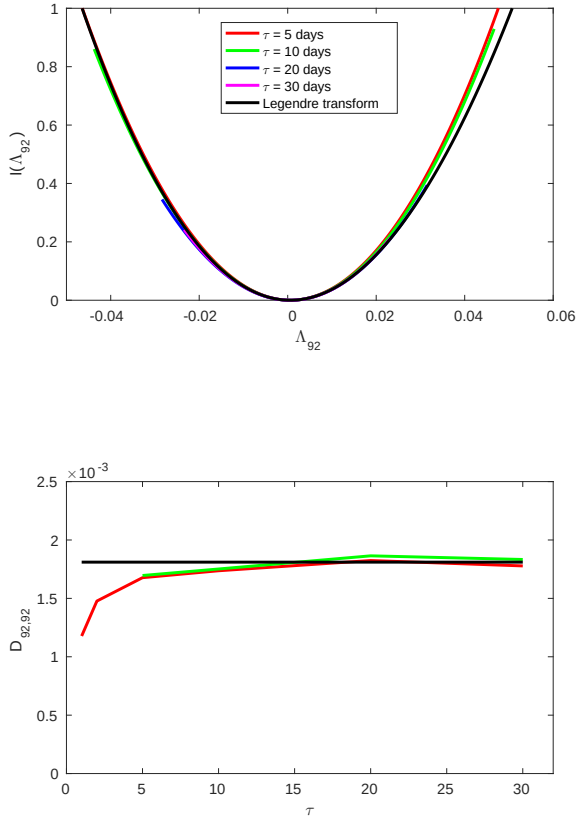

Figure 7. (a) Large-deviation rate function of the 92th finite-time Lyapunov exponent. (b) Element $D_{92,92}$ of the diffusion matrix as estimated from the time series of finite-time Lyapunov exponents (red), from the curvature of the large-deviation rate function derived from the probability density (green) and from the curvature of the large-deviation rate function derived with the Legendre transform (black).

tuate together in phase. The first and second mode also display (negative and positive, respectively) correlations between the most unstable and the highly stable FTLEs. These two modes are virtually independent of the integration time τ.

A large-deviation principle can be established for all of the FTLEs. The convergence to the large-deviation limit behaviour is quite fast, except for the most unstable exponents where it is slower. Also a joint large-deviation rate function for the first and the second FTLE is estimated. Good correspondance is found between the curvature of the large-deviation rate functions at the minimum and the corresponding elements of the diffusion matrix.

Competing interests. The author declares that they have no conflict of interest.

Nonlin. Processes Geophys. Discuss., https://doi.org/10.5194/npg-2018-25
Manuscript under review for journal Nonlin. Processes Geophys.
Discussion started: 2 May 2018

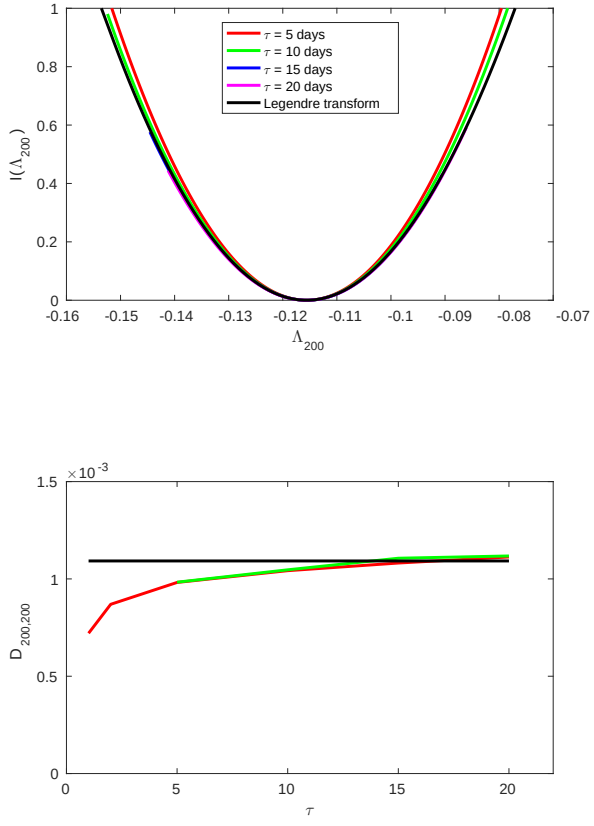

Figure 8. (a) Large-deviation rate function of the 200th finite-time Lyapunov exponent. (b) Element $D_{200,200}$ of the diffusion matrix as estimated from the time series of finite-time Lyapunov exponents (red), from the curvature of the large-deviation rate function derived from the probability density (green) and from the curvature of the large-deviation rate function derived with the Legendre transform (black).

References

Benettin, G., Galgani, L., Giorgilli, A., and Strelcyn, J.-M.: Lyapunov characteristic exponents for smooth dynamical systems and for Hamiltonian systems: a method for computing all of them. Part 1: Theory, Meccanica, 15, 9–20, 1980.

Eckmann, J., and Ruelle, D.: Ergodic theory of chaos and strange attractors, Reviews of Modern Physics, 57, 617–656, 1985.

Johnson, P. L. and Meneveau, C.: Large-deviation joint statistics of the finite-time Lyapunov spectrum in isotropic turbulence, Physics of Fluids, 27, 085110, 2015.

Kalnay, E.: Atmospheric Modeling, Data Assimilation, and Predictability, Cambridge University Press, 2003.

Kifer, Y.: Large deviations in dynamical systems and stochastic processes, Transactions of the American Mathematical Society, 321, 505–524, 1990.

Kuptsov, P. V. and Politi, A.: Large-deviation approach to space-time chaos, Physical Review Letters, 107, 114101, 2011.

Kwasniok, F.: Reduced atmospheric models using dynamically motivated basis functions, Journal of the Atmospheric Sciences, 64, 3452–3474, 2007.

Laffargue, T., Lam, K.-D. N. T., Kurchan, J., and Tailleur, J.: Large deviations of Lyapunov exponents, Journal of Physics A: Mathematical and Theoretical, 46, 254002, 2013.

Legras, B., and Ghil, M.: Persistent Anomalies, Blocking, and Variations in Atmospheric Predictability, Journal of the Atmospheric Sciences, 42, 433–471, 1985.

Lorenz, E. N.: Deterministic Nonperiodic Flow, Journal of the Atmospheric Sciences, 20, 130–141, 1963.

Marshall, J. and Molteni, F.: Toward a dynamical understanding of planetary-scale flow regimes, Journal of the Atmospheric Sciences, 50, 1792–1818, 1993.

Oseledets, V. I.: A multiplicative ergodic theorem. Characteristic Ljapunov exponents of dynamical systems, Transactions of the Moscow Mathematical Society, 19, 179–210, 1968.

Ott, E.: Chaos in Dynamical Systems, Cambridge University Press, 2002.

Pikovsky, A. and Politi, A.: Lyapunov Exponents, Cambridge University Press, 2016.

Roads, J. O.: Predictability in the extended range, Journal of the Atmospheric Sciences, 44, 3495–3527.

Schubert, S., and Lucarini, V.: Covariant Lyapunov vectors of a quasi-geostrophic baroclinic model: Analysis of instabilities and feedbacks, Quarterly Journal of the Royal Meteorological Society, 141, 3040–3055, 2015.

Shimada, I. and Nagashima, T.: A Numerical Approach to Ergodic Problem of Dissipative Dynamical Systems, Progress of Theoretical Physics, 61, 1605–1616, 1979.

Touchette, H.: The large deviation approach to statistical mechanics, Physics Reports, 478, 1–69, 2009.

Vannitsem, S.: Predictability of large-scale atmospheric motions: Lyapunov exponents and error dynamics, Chaos, 27, 32101, 2017.

Vannitsem, S., and Lucarini, V.: Statistical and Dynamical Properties of Covariant Lyapunov Vectors in a Coupled Atmosphere-Ocean Model – Multiscale Effects, Geometric Degeneracy, and Error Dynamics, Journal of Physics A: Mathematical and Theoretical, 49, 224001, 2016.

Vannitsem, S., and Nicolis, C.: Lyapunov Vectors and Error Growth Patterns in a T21L3 Quasigeostrophic Model, Journal of the Atmospheric Sciences, 54, 347–361, 1997.

Nonlin. Processes Geophys. Discuss., https://doi.org/10.5194/npg-2018-25
Manuscript under review for journal Nonlin. Processes Geophys.
Discussion started: 2 May 2018

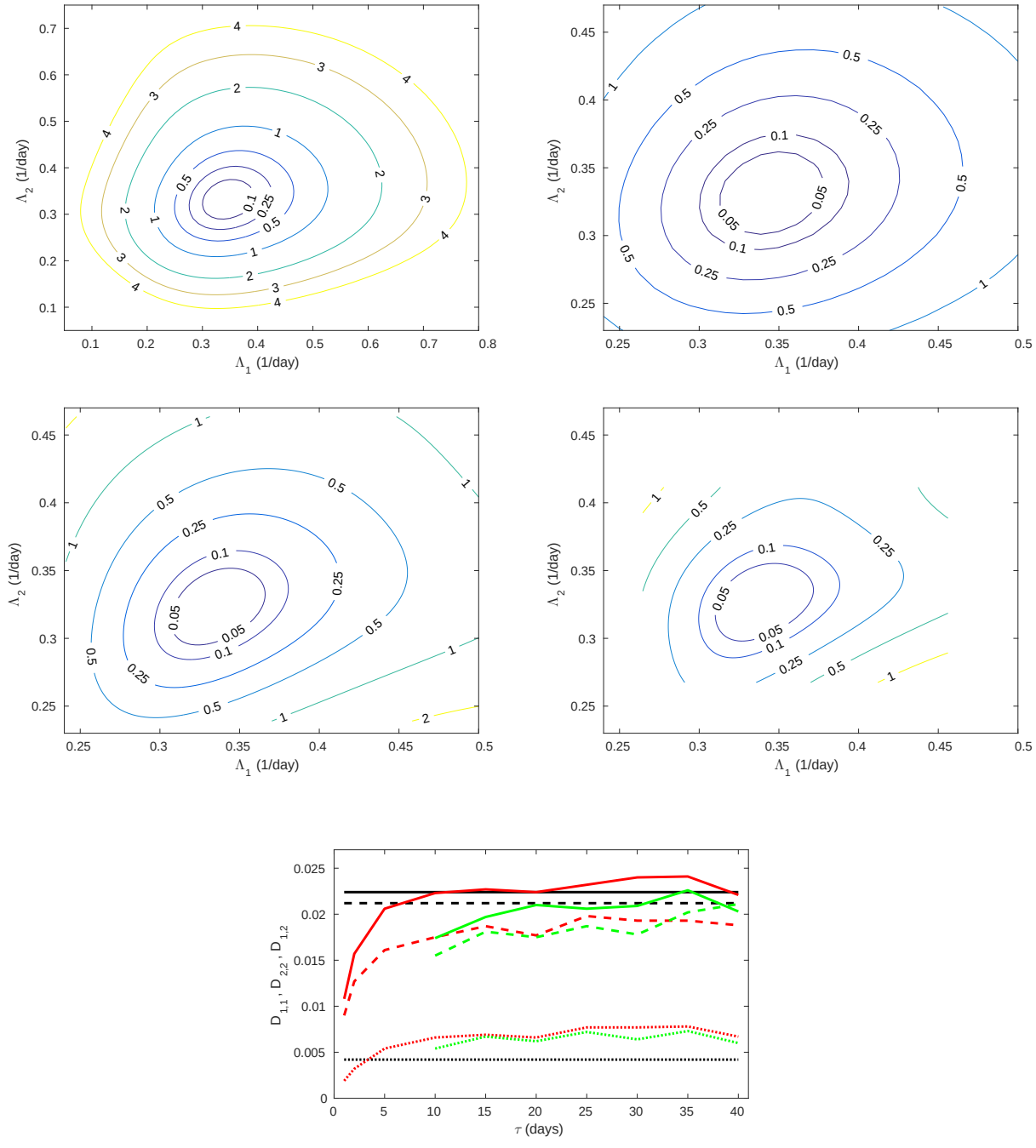

Figure 9. (a) Joint large-deviation rate function of the first two finite-time Lyapunov exponents as estimated with the Legendre transform. (b) Close-up of (a). (c) Joint large-deviation rate function as estimated from the probability density of the finite-time Lyapunov exponents for $\tau = 15$ days. (d) As (c) with $\tau = 30$ days. (e) Elements $D_{1,1}$ (solid), $D_{2,2}$ (dashed) and $D_{1,2}$ (dotted) of the diffusion matrix as estimated from the time series of the finite-time Lyapunov exponents (red), from the curvature of the joint large-deviation rate function derived from the probability density (green) and from the curvature of the joint large-deviation rate function derived with the Legendre transform (black).